Physical Conditions, Carbon Transport, and Climate Change Impacts in a Northeast Greenland Fjord

Authors: Rysgaard, Søren, Vang, Torben, Stjernholm, Michael, Rasmussen, Bjarke, Windelin, Anders, et al.

Source: Arctic, Antarctic, and Alpine Research, 35(3) : 301-312

Published By: Institute of Arctic and Alpine Research (INSTAAR), University of Colorado

URL: https://doi.org/10.1657/1523-0430(2003)035[0301:PCCTAC]2.0.CO;2

Arctic, Antarctic, and Alpine Research, Vol. 35, No. 3, 2003, pp. 301–312

Physical Conditions, Carbon Transport, and Climate Change Impacts in a Northeast Greenland Fjord

*Søren Rysgaard,**
Torben Vang,†
Michael Stjernholm,‡
*Bjarke Rasmussen,**
Anders Windelin,† and
Sissi Kiilsholm§

*Dept. Marine Ecology, National Environmental Research Institute, Vejlsøvej 25, 8600 Silkeborg and Frederiksborgvej 399, P.O. Box 358, 4000 Roskilde, Denmark.
Søren Rysgaard,
sr@dmu.dk
†Council of Vejle, Damhaven 12, 7100 Vejle, Denmark.
‡Dept. Freshwater Ecology, National Environmental Research Institute, Vejlsøvej 25, 8600 Silkeborg, Denmark.
§Danish Meteorological Institute, Lyngbyvej 100, 2100 Copenhagen Ø, Denmark.

Abstract

This paper presents data on physical conditions and carbon transport in a typical northeast Greenland fjord along with predictions of expected changes in the area due to climate change. The fjord has an average depth of 100 m; the maximum depth is 360 m, and a sill at a depth of 45 m is found at its entrance. Sea ice covers the fjord from early October to late July. The freshwater input to the fjord, occurring from June to September, is 1063×10^6 m^3 from the catchment area (3109 km^2) and 440×10^6 m^3 from melting of sea ice. During the ice-free period this buoyancy input and mixing by wind and tides results in an estuarine circulation in which lighter low-salinity water is moved seaward above denser water from the Greenland Sea. The tidal amplitude is 0.8 to 1.5 m, and the transport of tides from the outer parts of the fjord to the inner parts is delayed less than 15 min due to low friction in the fjord system. During the ice-free period, a net carbon input of 15–50 t C d^{-1} occurs in the outer region of the fjord due to transport from land and the adjacent Greenland Sea. A regional atmosphere-ocean model predicts a temperature increase of 6–8°C at the end of this century (2071–2100) that will lead to increase in freshwater runoff, thinning of the sea ice, and an increase in ice-free conditions from 2.5 mo to 4.7–5.3 mo in Young Sound. The increased freshwater input will greatly enhance the estuarine circulation and nutrient input to the fjord and is expected to increase biological productivity.

Introduction

Numerical simulations of future climate performed by use of general circulation models all agree that climate warming will occur first and most intensively in arctic and subarctic regions (e.g., Manabe and Stouffer, 1993; Cattle and Crossley, 1996; Shindell et al., 1999; Flato and Boer, 2001). Surface air temperature observations reveal that the largest increase in recent decades has occurred over Northern Hemisphere land areas from about 40 to 70°N (Serreze et al., 2000). Due to warming of the world oceans (Levitus et al., 2000) the sea-ice cover in the Arctic has decreased by ~14% since the 1970s (Johannessen et al., 1999). This decrease has led to a prolongation of the open-water period off the north coast of Russia and in the Greenland Sea, the Barents Sea, and the Sea of Okhotsk (Parkinson, 1992). Higher atmospheric temperatures will increase the transport of water vapor toward the North Pole, resulting in an increase in precipitation and freshwater supply to high latitudes. This prediction agrees well with the observed general increase in precipitation in the 55–85°N latitude band during the last century (Serreze et al., 2000).

The research and monitoring station ZERO (Zackenberg Ecological Research Operations) was established in 1995 in Young Sound, northeast Greenland, with a view to monitoring effects of climate changes in a high arctic environment. The study area is considered to be a sensitive indicator of climate change because of its contact with water masses from the Greenland Sea and direct meltwater flux from the Greenland Ice Sheet. It is believed that the predicted climate changes will dramatically alter the conditions in the Greenland Sea as well as coastal hydrological conditions. A long-term marine monitoring program will supplement the ongoing monitoring program of the terrestrial environment in 2003. Detailed quantitative studies of the marine ecosystem processes are being conducted in the area, including seasonal measurements of primary production by phytoplankton (Rysgaard et al., 1996, 1999), sea-ice microalgae (Kühl et al., 2001; Rysgaard et al., 2001; Glud et al., 2002a), brown algae (Borum et al., 2002), benthic microalgae (Glud et al., 2002b), and coralline red algae (Roberts et al., 2002). Furthermore, seasonal measurements of mineralization rates in the water column (Rysgaard et al., 1999; Levinsen et al., 2000) and within the sediment (Rysgaard et al., 1998; Glud et al., 2000; Berg et al., 2001) have been made, along with estimates of abundance and production of dominant infauna (Sejr et al., 2000; Sejr et al., 2002) and walrus abundance and predation (Born et al., 1997; Born et al., 2003). In an attempt to establish carbon and nutrient budgets and models for carbon and nutrient cycling in this high arctic fjord (Young Sound), detailed data on bathymetry and hydrographic conditions are needed.

In this study, we surveyed the bottom topography of Young Sound and combined the resulting data with existing topographical data from land to provide hypsometry and catchment data on the fjord. Young Sound is the first fjord in northeast Greenland to be fully surveyed, and our investigation covers climatic data, water discharge from the catchment area, and sea-ice conditions during 2000–2001, along with hydrographic conditions during the short summer thaw. We used a hydrodynamic model to evaluate the barotrophic signals entering Young Sound from the adjacent sea. The model is based on the topography, freshwater input, and wind conditions as input variables and is used to estimate water transport in the fjord. Furthermore, measurements of nutrients and total organic carbon in the water column are used in a volume-mass model to estimate a carbon budget for the outer fjord area. Finally, simulations of future changes in climatic conditions using a regional climate model are presented and discussed in relation to expected changes in the ice-free period, water discharge, and hydrographic conditions in Young Sound.

1523-0430/03 $7.00

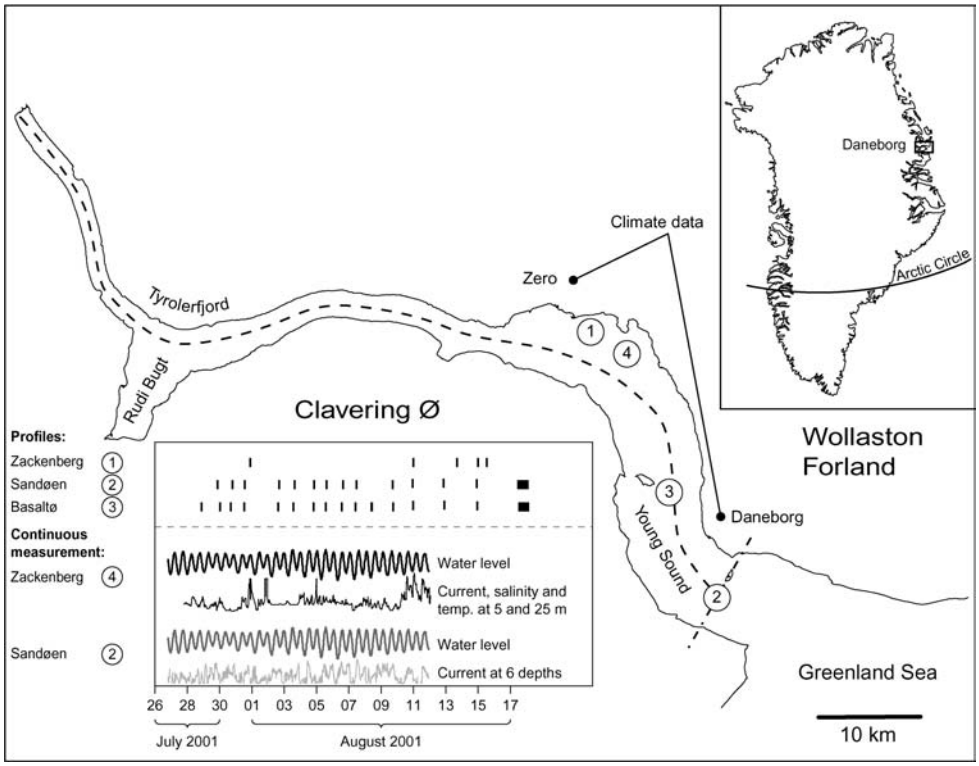

FIGURE 1. Meteorological and hydrographic measuring stations in Young Sound used in this investigation. Numbers 1, 2, 3, and 4 refer to the different measuring stations as shown in the inserted box. Profiles of temperature, salinity, TOC, TN, and nutrients were made regularly throughout the measuring campaign, as illustrated by small vertical ticks. Note the intensive sampling at the end of the period. Continuous measurements of water level, salinity, and temperature were made at 2 locations, 2 and 4. Broken line represents sites of salinity and temperature mapping (CTD profiles), along and across Young Sound.

Methods

STUDY AREA

This investigation was carried out in the fjord Young Sound (74°18′N, 20°18′W) situated in the Northeast Greenland National Park (Fig. 1). Long-term climatic records (1958–1999) are available from Daneborg, situated in the outer part of the fjord (Cappelen et al. 2001), and from Zackenberg Ecological Research Operations (1995–present) located farther inside the fjord (Meltofte and Thing, 1996, 1997; Meltofte and Rasch, 1998; Rasch, 1999). The duration of the midnight sun and polar night periods in the area is 101 days and 81 days, respectively, with a maximum incoming radiation of ~800 W m^{-2} during summer (Fig. 2a). Winters are generally very cold, with mean monthly temperatures as low as –22°C (Fig. 2b). Mean temperatures (1961–1999) are below freezing 9 months of the year, and only the months June to August have positive mean air temperatures of up to 4.0°C. During summer the outer area of Young Sound is often affected by fog from the ice-filled sea, the temperature of the fog being only a little above 0°C. The mean annual wind velocity (1958–1999) in the area is 4.9 m s^{-1}, most frequently coming from the north (Fig. 2c). However, during June–August (1958–1999) the dominant wind direction is easterly, with a mean wind velocity of 4.1 m s^{-1}. Annual precipitation varies from 214 to 320 mm, approximately 75% of which is snow (Ohmura and Reeh, 1991; Soegaard et al., 2001). Snow cover is usually formed in September and disappears through June–July. Fast ice in the fjord breaks in July, and new ice begins to form in September, growing to a thickness of 10–15 cm in early October (Fig. 2d).

BATHYMETRY

The outer part of the fjord (Glud et al., 2000) and an area near Zackenberg (Nielsen and Rasch, 1997) have been mapped earlier using a relatively coarse net of transects. In this study, we improved data cover in these areas as well as surveying the bottom topography of the remaining part of Young Sound. In particular, the outer part of the sound around the sill was mapped in great detail. The survey was performed from a rubber dinghy using a dual-frequency echo sounder and GPS receiver. Data were recorded continuously along predefined transects. The surveyed transects totaled 850 km, and a total of 200000 data points was collected. These data were integrated with the topographical data from the Geological Survey of Denmark and Greenland (GEUS) and a Landsat TM satellite image to construct a map of the entire area. This combined data set was used to estimate the catchment area of Young Sound.

The freshwater discharge from the Zackenberg River has been available since 1995 from automatic water-level recordings and frequent discharge measurements (Rasch et al., 2000).

HYDROGRAPHIC MEASUREMENTS

Continuous measurements of water level, salinity, temperature, current velocity, and direction were made at water depths of 5 and 25 m at 2 positions using Aanderaa RCM 9 current meters (Aanderaa instruments, Bergen, Norway). One station was placed at the mouth of the fjord near the small island of Sandøen (74°14.995′N, 20°11.111′W), and the other about 30 km upstream near Zackenberg (74°26.450′N, 20°27.157′W). These stations will be referred to as the Sandøen station and the Zackenberg station, respectively (Fig. 1b). We made additional measurements using an Aanderaa DCM 12 current profiler near Sandøen (Aanderaa instruments, Bergen, Norway). This instrument, an Acoustic Duppler Current Profiler (ADCP), continuously measures the current velocity and direction at 6 water depths as well as the water levels.

Daily measurements of water temperature and salinity profiles (0–100 m) were made using a Conductivity Temperature Detector (CTD) profiler (SIS CTD + 100) together with daily samplings of water (1, 5, 10, 15, 20, 30, and 50 m) from 2 stations: the Sandøen station and the Basaltø station (74°19.336′N, 20°19.828′W) situated near the island of Basaltø (Fig. 1). During a tidal period at the end of the field program, hourly CTD profiles were recorded and water samples collected in the

same depth intervals at which daily measurements were made. We also conducted length and cross-section measurements of salinity and temperature profiles in the fjord. Salinity was measured using the Practical Salinity Scale, and all sensors were calibrated immediately after the field campaign.

Water samples for determination of NO_3^- and PO_4^{3-} were filtered through glass fiber filters (Whatman GF/F) and frozen (–18°C) within 1–3 h after collection in the field. Samples for total organic carbon (TOC) and total nitrogen (TN) determinations were frozen in acid-washed 30-ml vials for later analysis. Concentrations of $NO_3^- + NO_2^-$ were determined according to the scheme of Braman and Hendrix (1989). Phosphate and TN concentrations were determined by standard methods as described by Grasshoff et al. (1983). TOC was analyzed with a Shimadzu TOC-5000 Analyser using high-temperature catalytic techniques described in Buesseler et al. (1996). TOC calibrations were made with 45-µl injections of $C_8H_5KO_4$ in UV-oxidized Q-water. All carbon data were corrected for instrument blank of 12 µM, and each measurement represents the mean of 3 to 7 injections.

Results

Young Sound covers an area of 390 km^2 and is ~90 km long and 2–7 km wide (Fig. 3). The volume of the fjord is 40 km^3, and the average depth in the fjord is ~100 m, the maximum depth of 360 m being found in Tyrolerfjord (Region 4). A 45-m sill is found in the outer part of the fjord and another further inside the fjord (Region 5). Sea-floor area and volume of the different regions (0–6) are given in Tables 1 and 2, respectively.

The topographic map was used to measure the catchment area of Young Sound (Fig. 4). The area was found to be 3109 km^2, although the borders of the watershed on the Inland Ice sheet are uncertain. Water discharge from the Zackenberg River peaked at 60 $m^3\ s^{-1}$ around 30 June (Fig. 5). The total water discharge in 2001 was 175×10^6 m^3, and 65% occurred from 8 June to 20 July. The values for 1997, 1998, and 1999 were 174×10^6, 256×10^6, and 186×10^6 m^3, respectively. Assuming that the water discharge in the Zackenberg River, representing a catchment area of 512 km^2 (Rasch et al., 2000), is representative of the entire Young Sound catchment area (3109 km^2), the total water discharge to the fjord is 1063×10^6 $m^3\ yr^{-1}$.

Sea ice in the fjord represents a maximum freshwater input of 540×10^6 m^3, in the event that all ice within the fjord should melt. However, the sea ice broke on 27 July 2001 (Fig. 2d), when it was around 20–30 cm thick, and was exported from the fjord to the Greenland Sea within 1 d. This export represents $\sim 100 \times 10^6$ m^3 fresh water. Drifting sea ice was absent from Young Sound until 11 August, when dense pack ice suddenly entered Young Sound and drifted within the fjord for 1–2 d before being exported to the Greenland Sea once again. Regular sea ice was established again by early October.

Young Sound is a deep-sill fjord with significant buoyancy input in the form of fresh water from the melting of snow and ice in the catchment area and the melting of sea ice. During the ice-free period, the freshwater input and mixing by wind and tides results in an estuarine circulation, where lighter water of salinity <30 is moved seaward above denser water from the East Greenland Current with a salinity of 31.5–33 (Fig. 6). The primary pycnocline is found at a depth of 5 m, and the surface-layer salinity is in the range of 14–30 (Fig. 6). The freshwater content above the sill depth decreases gradually from 0.07 in the Tyrolerfjord to 0.026 at Basaltøen and 0.014 at Sandøen. The temporal variation at Basaltøen and Sandøen causes the errors of the mean freshwater content to be 0.002 and 0.004, respectively. However, the surface-layer temperature is 2–7°C and reaches 6–7°C in the inner parts of the fjord (Fig. 7). The density difference across the pycnocline has a magnitude of 5–10 kg m^{-3}.

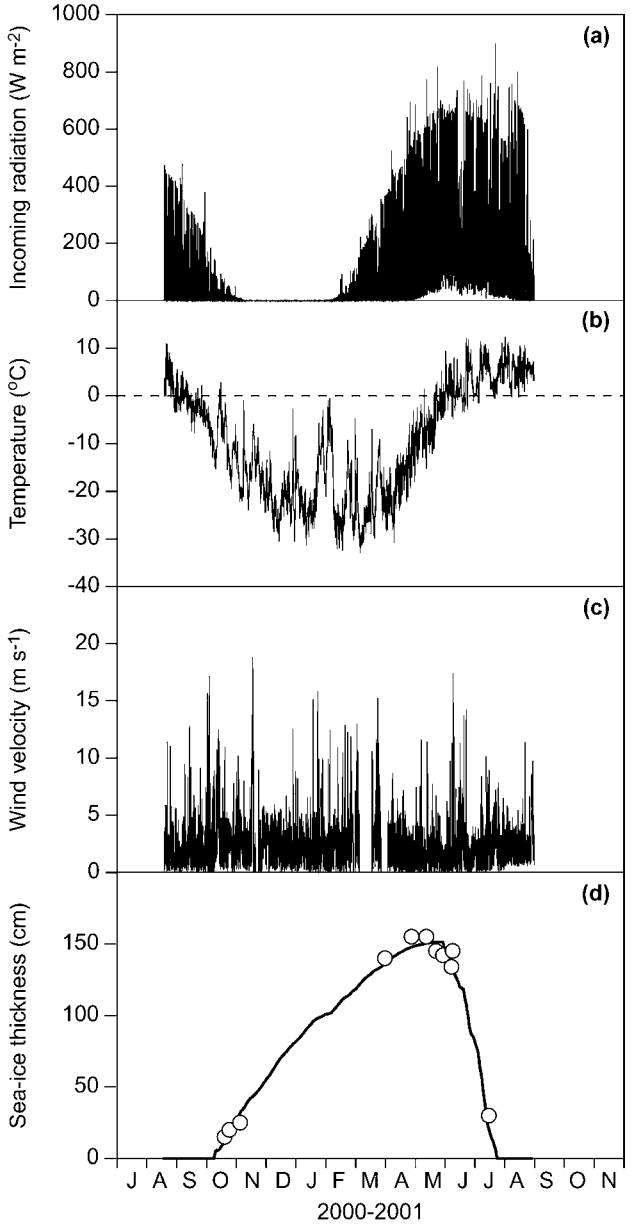

FIGURE 2. Climatic conditions and sea-ice cover in Young Sound during 2000–2001: (a) incoming radiation, (b) temperature, (c) wind velocity, and (d) measured sea-ice thickness (dots) and estimated thickness (line) calculated from Lebedev (1938) and Biello (1961, 1980).

At larger depths salinity increases while temperatures are below zero. The subzero temperature zone gradually deepens farther inside the fjord (Fig. 7b). The cool and more saline water from the Greenland Sea submerges below the surface water of Young Sound, and weak tidal mixing decreases its salinity and increases its temperature by entrainment of warmer low-salinity surface water. The horizontal density differences caused by differences in salinity exceed those caused by temperature. Consequently, the baroclinic circulation is dominated by differences in salinity.

A tidal amplitude of 0.8 to 1.5 m was observed at both the Sandøen and Zackenberg sites (Fig. 8a). A hydrodynamic model simulation of tidal amplitude agreed well with the measured data set on both monthly (Fig. 8a) and diurnal (Fig. 8b) scales. Furthermore, the model predicted high current velocities at the entrance to the fjord between Sandøen and Clavering Ø (Fig. 8c) in an area where polynyas

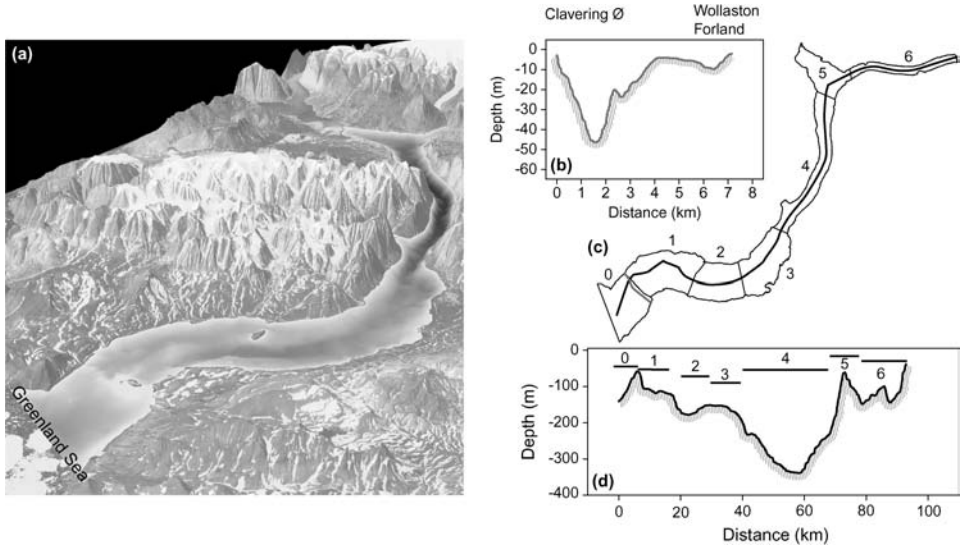

FIGURE 3. (a) Relief model of Young Sound. (b) Cross-section at the sill in the outer part of Young Sound. (c) Young Sound was divided into 7 regions (see Tables 1 and 2), where region 0 and 1 have been intensively studied in the CAMP project. (d) Length section of the fjord with marking of regions.

are observed regularly (Fig. 8d). Direct measurement shows surface current velocities of up to 120 cm s^{-1} near Sandøen, with a mean velocity of 45 cm s^{-1}. Calculations of the currents revealed that the mean velocity in the entire cross-section at Sandøen is 17 cm s^{-1}. Inside Young Sound the mean velocity is lower by a factor 10 because the barotrophic flow is distributed over a larger cross-sectional area compared to the area at the entrance of the fjord.

During the study period, the TOC concentration in the water column ranged from approximately 60 to 110 μM at the Sandøen and Basaltø sites (Fig. 9a). Elevated concentrations were found in the upper 10–25 m in association with the pycnocline in the period 2–12 August. TN concentrations ranged from 5–15 μM at the Sandøen station and 8–20 μM at the Basaltø station, with an average TOC:TN ratio of 9 at both stations (data not shown). Nitrate concentrations ranged from 0–4 μM in the upper 50 m of the water column, with values below 0.5 μM in the upper 10–25 m (Fig. 9b). A vertical concentration gradient of PO_4^{3-} was also observed at the two sites during the study period, with concentrations below 0.3 μM in surface waters and up to 1.5 μM around a depth of 50 m (Fig. 9c).

Discussion

BATHYMETRY

Young Sound is an East Greenland fjord similar to numerous other large and deep fjords in the region that often penetrate hundreds of km inland (Fig. 3). The fjords are typically U-shaped valleys incised into high mountain plateaus and continuing westward underneath the Greenland Ice Sheet (Sugden, 1974). With lengths of up to 300 km and depths to 1600 m, the East Greenland fjords are among the longest and deepest in the Northern Hemisphere (Funder et al., 1998; Cofaigh et al., 2001). The Young Sound–Tyrolerfjord system is narrow and steep-walled in its interior (Tyrolerfjord) and wider and more shallow toward the mouth (Young Sound) (Fig. 3). This topographical contrast is typical of glacially eroded fjords (Bennet and Glasser, 1996) but has become more prominent in the Young Sound–Tyrolerfjord system due to differences in bedrock geology between the inner part of the fjord, consisting of hard Caledonian gneisses, and the outer part of the fjord, of softer Cretaceous and Tertiary basalts and sandstones (Escher and Watt, 1976). Although data on bathymetry in fjords along the East Greenland

TABLE 1

Sea-floor area (km^2) in given depth internals in Young Sound

Depth Interval (m)	Region 0	Region 1	Region 2	Region 3	Region 4	Region 5	Region 6	Total (0–6)
0–10	9.827	5.324	1.479	3.521	1.913	3.512	1.473	27.049
10–20	3.958	3.136	1.610	2.578	1.741	2.407	1.424	16.853
20–30	3.427	3.405	1.757	2.465	1.677	2.281	1.469	16.480
30–40	3.288	3.630	1.800	2.509	1.682	2.228	1.528	16.664
40–50	3.828	3.863	1.917	2.558	1.641	2.271	1.585	17.661
50–60	4.668	4.776	2.328	2.308	1.642	2.803	1.680	20.204
60–70	3.868	5.456	2.813	2.452	1.547	2.361	2.063	20.559
70–80	4.078	7.678	3.349	2.770	1.506	1.988	2.098	23.465
80–90	4.139	10.111	5.404	3.036	1.539	1.688	2.052	27.968
90–100	4.214	8.888	3.979	3.425	1.495	1.601	2.320	25.921
100–120	8.263	13.036	6.323	7.574	2.984	2.878	5.083	46.141
120–140	5.274	2.782	7.338	8.724	3.106	3.114	3.761	34.100
140–160	0.929	2.452	7.012	12.600	3.331	3.735	1.299	31.358
160–180	0.000	1.609	6.057	5.026	3.609	2.694	0.172	19.167
180–200	0.000	0.000	0.343	1.706	3.999	2.005	0.010	8.062
200–250	0.000	0.000	0.000	0.305	13.754	4.204	0.000	18.263
250–300	0.000	0.000	0.000	0.000	11.813	0.000	0.000	11.813
300–360	0.000	0.000	0.000	0.000	7.637	0.000	0.000	7.637
Total area	59.759	76.144	53.508	63.556	66.615	41.767	28.016	389.366

TABLE 2

Volume (km^3) in given depth internals in Young Sound

Depth Interval (m)	Region 0	Region 1	Region 2	Region 3	Region 4	Region 5	Region 6	Total (0–6)
0–10	0.556	0.734	0.529	0.616	0.657	0.399	0.273	3.764
10–20	0.484	0.694	0.513	0.589	0.639	0.372	0.259	3.550
20–30	0.448	0.662	0.496	0.563	0.622	0.348	0.245	3.385
30–40	0.414	0.627	0.479	0.539	0.605	0.326	0.230	3.219
40–50	0.380	0.590	0.460	0.513	0.589	0.303	0.214	3.048
50–60	0.338	0.548	0.440	0.489	0.572	0.278	0.198	2.863
60–70	0.294	0.496	0.414	0.465	0.556	0.252	0.180	2.657
70–80	0.255	0.433	0.384	0.440	0.541	0.230	0.158	2.440
80–90	0.214	0.346	0.342	0.411	0.526	0.211	0.138	2.187
90–100	0.172	0.245	0.291	0.378	0.511	0.195	0.116	1.909
100–120	0.219	0.266	0.478	0.650	0.977	0.345	0.155	3.089
120–140	0.072	0.104	0.349	0.489	0.916	0.288	0.064	2.281
140–160	0.004	0.061	0.196	0.269	0.851	0.214	0.013	1.608
160–180	0.000	0.010	0.066	0.084	0.783	0.151	0.002	1.095
180–200	0.000	0.000	0.001	0.020	0.707	0.104	0.000	0.832
200–250	0.000	0.000	0.000	0.002	1.341	0.079	0.000	1.422
250–300	0.000	0.000	0.000	0.000	0.679	0.000	0.000	0.679
300–360	0.000	0.000	0.000	0.000	0.169	0.000	0.000	0.169
Total volume	3.849	5.816	5.437	6.517	12.240	4.095	2.245	40.199

coast are sparse (e.g., Cofaigh et al., 2001; this study) it is likely that most of the fjords have one or more sills (Funder, 1989; Funder and Hansen, 1996; Funder et al., 1998). As the presence of sills restricts horizontal water exchange along the longitudinal axis of the fjord, variations in bathymetry and water depth at the sill between fjords will lead to different water-exchange conditions from one fjord to another, as has been shown in Norwegian fjords (Aure and Stigebrandt, 1989).

HYDROGRAPHY

Typically, meltwater from the Inland Ice and/or rivers drain into the inner parts of the East Greenland fjords. The total freshwater discharge in Young Sound takes place over a 3-mo period during June–September, when air temperatures exceed 0°C, and 65% of the discharge occurs within 6 wk in 2001 (Figs. 2b, 5). The outflow of fresh water and mixing result in a seaward surface slope and also causes the primary pycnocline in the depth range 5–10 m (Fig. 6) to have a landward inclination.

Evaluation of the tidal current and circulation using the 2D hydrodynamic model (MIKE21, DHI, Hørsholm, Denmark) showed that transport of tides was delayed less than 15 min from the mouth of Young Sound to the Zackenberg station due to low friction in the fjord system (Fig. 8). Thus, the energy loss of the barotrophic signal is minimal. However, the tidal forces generate high current velocities (up to 120 cm s^{-1}) at the mouth of Young Sound, causing a delay in establishment of ice cover in the outer sill area (Fig. 8). Openings (polynyas) in the sea ice have regularly been observed to form in this area during winter and may in some cases initiate a larger opening from

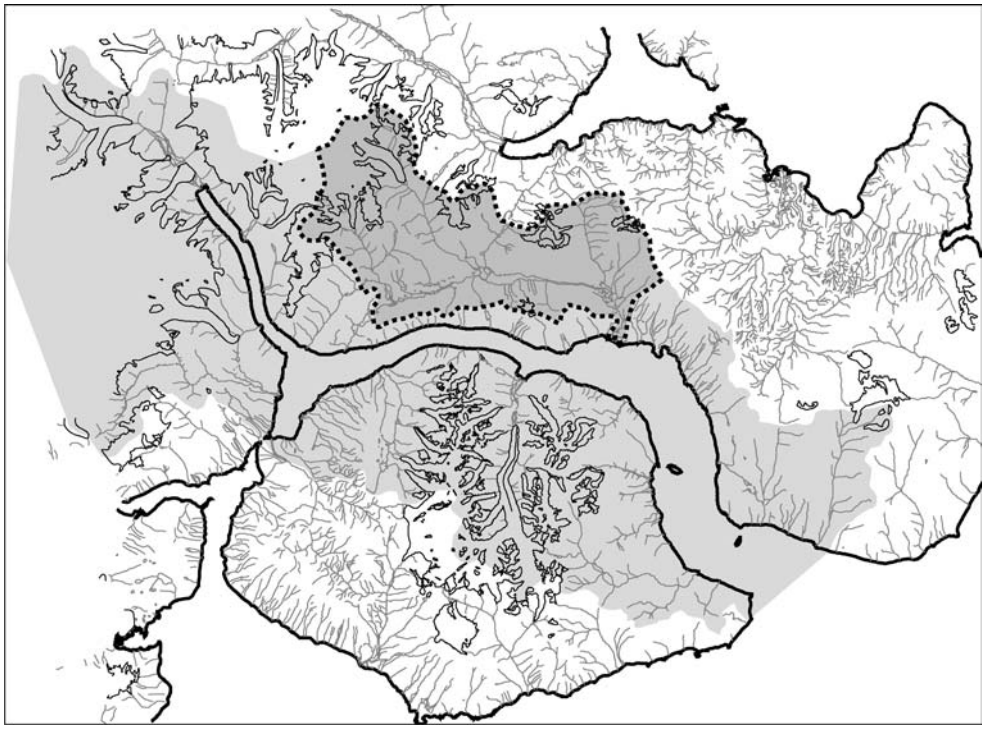

FIGURE 4. Catchment area of Young Sound showing the drainage basin of the Zackenberg River (dotted outline).

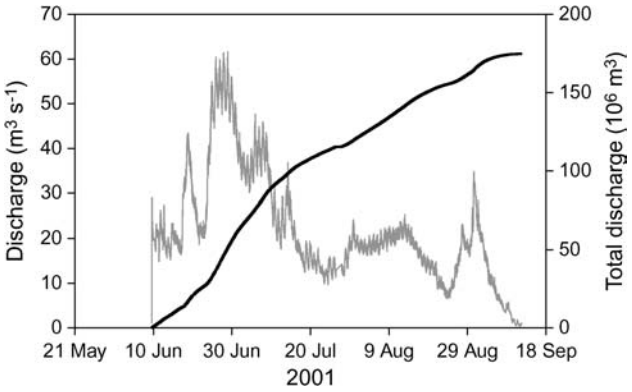

FIGURE 5. Water discharge from the Zackenberg River.

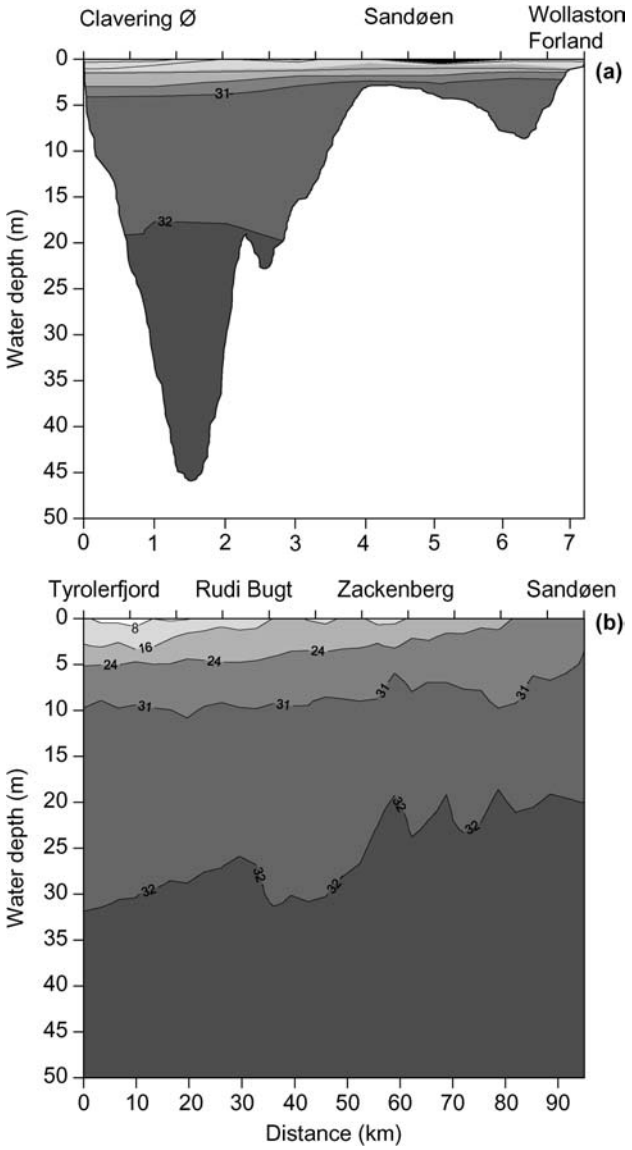

FIGURE 6. Salinity across the sill in the outer part of the fjord area (a) and along Young Sound (b). The horizontal and vertical resolutions of measurements are (a) 0.5 km and 20 cm and (b) 2 km and 20 cm, respectively.

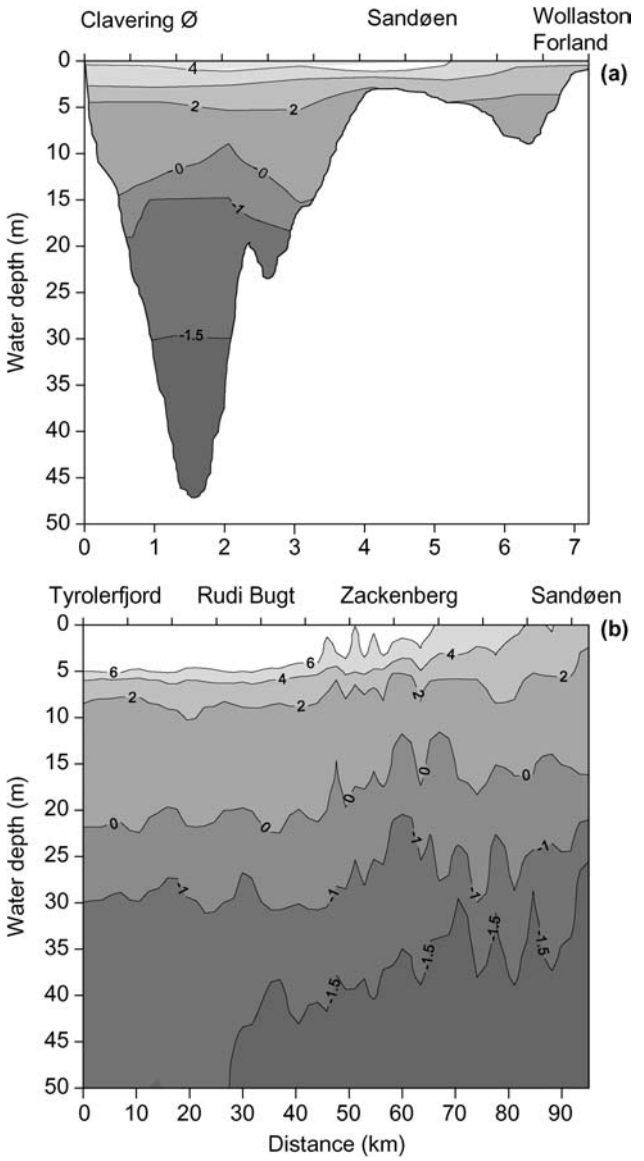

FIGURE 7. Temperature (°C) conditions (a) across the sill in the outer part of the fjord and (b) along Young Sound. The resolution of measurements as in Fig. 6.

the Sandøen location and several km inside the fjord (Military Division Sirius, personal communication).

During summer, current velocities have a magnitude of 0.05 m s^{-1}, while the mean wind velocity is 4.9 m s^{-1}. This represents a production of turbulent kinetic energy of 0.1×10^{-3} W m^{-2} and 5.6×10^{-3} W m^{-2}, respectively. The energy produced by wind is calculated according to the procedure of Rasmussen (1997), while the tidal production is calculated as a bottom shear stress times the average tidal velocity applying a friction coefficient of 10^{-3}. The wind mixing may support an entrainment from below the pycnocline of 6.4×10^{-7} to 1.3×10^{-6} m s^{-1} at the present surface-layer thickness (5 m) and the density difference across the pycnocline (5–10 kg m^{-3}). However, the quantities suggest that during the ice-free period, wind forcing is the dominant mixing agent of the surface waters, while tidal mixing and internal waves give rise to mixing in the deeper areas of Young Sound. Little change in density was seen in the water mass below a depth of 25–30 m during this investigation. At the entrance to Young Sound, tidal currents are stronger and have a strong influence on the mixing of the surface layer.

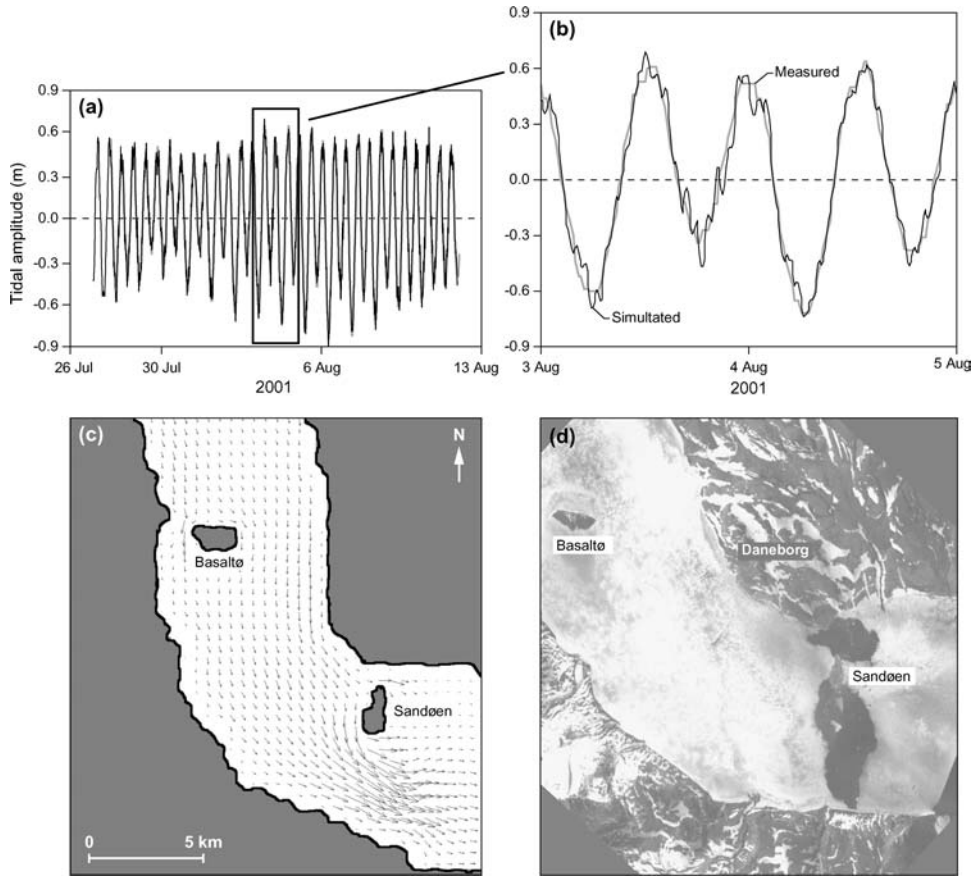

FIGURE 8. Measured and modeled water level in July–August (a). Measured and modeled water level from 3–5 August (b). Model output of current conditions in outer Young Sound (c). Satellite photo of sea-ice conditions in the same area in mid-October 2001 (d).

In the period of ice cover, wind mixing is absent, while both internal waves and tides mix the water column of Young Sound. Earlier measurements of salinity and temperature in bottom and surface waters during winter (February) have revealed a well-mixed water column (Rysgaard et al., 1999). Thus, total or partial renewal of the water in Young Sound most likely occurs during autumn, when stratification weakens due to cooling of surface waters and reduced freshwater inflow from the surrounding land, as observed in northern Norwegian sill basins (Eilertsen et al., 1981). In addition, the development of sea ice leads to formation of high-density brine that sinks toward the bottom, resulting in buoyancy-driven circulation. It has recently been demonstrated that brine leaking out of sea ice under freezing conditions is supersaturated with respect to O_2 (Glud et al., 2002a). Brine drainage may therefore also be responsible for a transfer of oxygenated water to deeper water layers. Thus, Young Sound belong to the "Arctic circulating category" presented in the model by Gilbert (1983) where mixing and permanently oxic conditions to the bottom is typical of fjords in the Canadian Arctic and west Greenland and give rise to rich and diverse benthos communities (Dale et al. 1989).

NUTRIENTS, TOTAL CARBON, AND NITROGEN

Irradiance causes the upper water layers to reach temperatures of 6–7°C (Fig. 7). Irradiance is sufficient to increase the temperature down to depths of 20 m (light attenuation is 0.19 m^{-1}). The irradiance further stimulates primary production to deplete NO_3^- within this depth range, while the concentration of PO_4^{3-} is only marginally reduced above the second pycnocline (Fig. 9). Nitrogen fixation has been shown to be of minor importance in the fjord (Rysgaard et al., 1996), and according to the Liebig's classical way of evaluating nutrient limitation through comparison of observed P:N concentrations with the Redfield ratio, 16N:1P, the very low NO_3^-:PO_4^{3-} ratio in the upper 20 m observed during the present investigation (Fig. 9b and c) supports earlier conclusions that NO_3^- limits primary production in the fjord (Rysgaard et al., 1999). The finding that phosphorus was present in excess throughout our investigation is also in accordance with observations from arctic waters in general (e.g., Harrison and Cota, 1991).

The elevated TOC concentrations found in the upper 10–25 m in association with the second pycnocline from 2–12 August (Fig. 9a) reflect increased chlorophyll values due to the onset of primary production following sea-ice breakup, as shown earlier at the same location (Rysgaard et al., 1999). This finding is further supported by the low TOC:TN ratio of 9 observed in the water column. The increase in nutrient concentrations below 10–25 m (Fig. 9b and c) is due to bacterial nutrient regeneration in the water column (Ottosen et al., unpublished data) and sediment (Rysgaard et al., 1998; Glud et al., 2000). In these previous studies from Young Sound it have been shown that nutrients (NO_3^-, NH_4^+, urea, PO_4^{3-}, and Si) were released from the sediment to the overlying water throughout the year due to active mineralization in the sediment.

CARBON TRANSPORT

Earlier investigations from the outer region of Young Sound suggest that mineralization exceeds primary production, and as such the system is net heterotrophic, requiring additional carbon input to balance mineralization (Glud et al., 2000, 2002b). The previous mass-balance study was based on direct measurements of primary production and mineralization in the pelagic and benthic compartments and vertical export and burial within the sediment. In order to make an independent estimate of the net heterotrophic versus net autotrophic status of Young Sound, a net carbon budget for the outer fjord area was established using techniques independent of the previous studies (Fig. 10). The

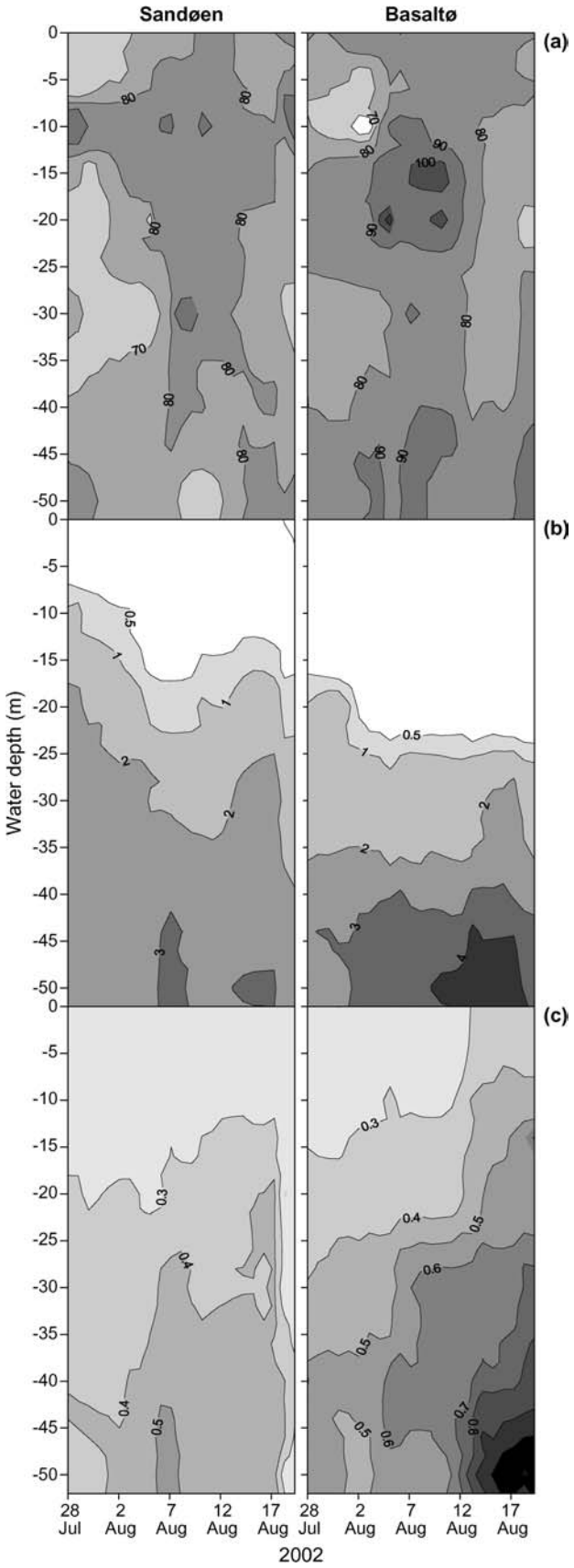

FIGURE 9. Vertical concentration profiles of TOC (a), nitrate (b), and phosphate (c) in the upper 50 m of the water column in Young Sound, 28 July–22 August. The maps are based on daily samplings from depths of 1, 5, 10, 15, 20, 30, and 50 m; units are in μM.

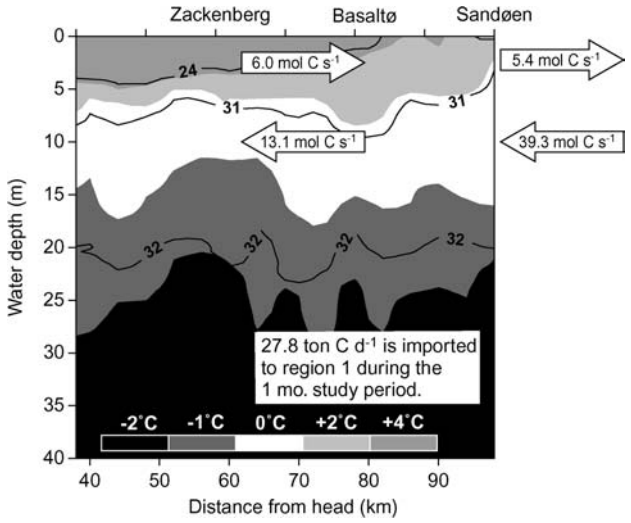

FIGURE 10. Carbon budget of outer area of Young Sound. Upper arrows represent the outward transport of carbon (TOC) due to freshwater volume flow. Lower arrows illustrate the inward TOC transport due to saltwater exchange. In total, 27.8 t C d^{-1} is imported to Region 1 between Basaltø and Sandøen cross-sections during the ice-free study period.

carbon export toward the sea (N_c, mol s^{-1}) was estimated through two separate transects (Sandøen and Basaltø—Fig. 3, region 1) as:

$$N_c = C_S R + (C_S - C_b)Q \quad (1)$$

where C_s is the TOC concentration in the outflowing surface-water mass; C_b is the concentration in the inflowing water; R is the freshwater volume flow; and Q is the saltwater transport, expressed as a volume flow although it also comprises dispersive transport, as estimated from a volume and salt-balance approach (e.g., Knudsen, 1900; Officer, 1980; Rasmussen and Josefson, 2002). The saltwater transport is calculated as:

$$Q = R/f \quad (2)$$

where f is the observed freshwater fraction at the cross-section. The steady-state assumptions in the Knudsen equations are fulfilled fairly well as the freshwater supply and mixing terms did not exhibit large temporal variability during this investigation (28 July–20 August). Furthermore, it takes the freshwater sources approximately 3 wk to supply the amount of fresh water found in Young Sound, and our budget is made on data collected 7 wk after runoff from land and after melting of sea ice started (Figs. 2, 5). Equations 1 and 2 are used to calculate the transports through the Sandøen and Basaltøen cross-sections (Fig. 3, Region 1). Thus, the transport in the Sandøen cross-section becomes:

$$N_{c,S} = (C_{s,S} + (C_{s,B} - C_{b,S})/f_S)R \quad (3)$$

and the transport in the Basaltøen cross-section becomes:

$$N_{c,B} = (C_{s,B} + (C_{s,B} - C_{b,B})/f_B)R \quad (4)$$

The difference between the transports at the Sandøen and Basaltø cross-sections then yields the net budget for the outer part of Young Sound:

$$NET = (C_{s,S} - C_{s,B} + (C_{s,S} - C_{b,S})/f_S - (C_{s,B} - C_{b,B}/f_B)R \quad (5)$$

When *NET* is less than zero, retention of TOC takes place in Region 1 in the outer part of the fjord. The validity of transports and net budget estimates is highly dependent upon the accuracy of the freshwater supply (R) and the facts that the observed TOC concentration

TABLE 3

Mean values and uncertainties in model parameters for estimating carbon transport in Region 1

	Mean	Standard error/Expected	n
$C_{s,S}$	71.80 mmol m^{-3}	3.10	48
$C_{b,S}$	79.13 mmol m^{-3}	1.95	116
$C_{s,B}$	79.54 mmol m^{-3}	3.46	39
$C_{b,B}$	84.09 mmol m^{-3}	2.28	110
f_S	0.014	0.009	25
f_B	0.026	0.019	19
R	75 m^3 s^{-1}	50–150 m^3 s^{-1}	

differences are large and the water-exchange parameters (f_B and f_S) reasonable. The magnitudes of the involved parameters as well as their uncertainties are presented in Table 3. The freshwater runoff from the catchment area of Young Sound is estimated at 75 m^3 s^{-1} during the investigation period, using discharge data from the Zackenberg River (Fig. 5) and adjusting for catchment area (Fig. 4). At the Sandøen cross-section, the freshwater-driven TOC export from the fjord ($C_{s,S}$ R) is 5.4 mol C s^{-1} is lower than the TOC import from the Greenland Sea arising from the concentration difference and the saltwater exchange ($(((C_{s,S}-C_{b,S})/f_S)R = -39.3$ mol C s^{-1}). Note that the negative value represents an import into the fjord. Consequently, the TOC flow is directed into the fjord at the Sandøen cross-section (Fig. 10). At the Basaltø cross-section, we find that the freshwater-driven TOC transport ($C_{s,B}$ $R = 6.0$ mol C s^{-1}) into Region 1 is lower than the flux out of Region 1 caused by the saltwater exchange ($(((C_{s,B}-C_{b,B})/f_B)R = -13.1$ mol C s^{-1}) and, hence, the TOC transport is directed away from Region 1 and further into the fjord (Fig. 10).

Bringing the calculation one step further toward the net budget, Equation 5 enhances the dependency of the concentration differences and estimated parameters (f_B and f_S). The net flux of TOC to Region 1 related to the freshwater volume flow ($(C_{s,S}-C_{s,B})R$) is –0.6 mol C s^{-1} which corresponds to a net retention of 0.6 mol C s^{-1} in Region 1 (Fig. 10, Table 1). Furthermore, the net flux of TOC into Region 1 from saltwater exchange ($(C_{s,S}-C_{b,S})/f_S - (C_{s,B}-C_{b,B})/f_B)R$ is –26.2 mol C s^{-1} corresponds to a net retention of 26.2 mol C s^{-1} in Region 1. In total, the net retention becomes 26.8 mol C s^{-1}, corresponding to 27.8 t C d^{-1} for Region 1 (Fig. 10).

This mass and volume budget supports previous findings of a net consumption of carbon in the outer part of Young Sound (Glud et al., 2000). However, it is difficult to assess the accuracy of this net carbon consumption estimate (–26.8 mol C s^{-1}) because of the uncertainty associated with the freshwater supply to the fjord. In the calculations of the total freshwater input to the fjord from the surrounding land, we assumed that the Zackenberg catchment area of 512 km^2 is representative of the entire catchment area of 3109 km^2 (Fig. 4). This estimate, though crude, is the best estimate at present because of the limited data available from other areas than the Zackenberg catchment area. If the freshwater input is subject to an uncertainty of 50%, the net carbon consumption (–26.8 mol C s^{-1}) will be in the range of 15–50 mol C s^{-1}, corresponding to 15–50 t C d^{-1} to Region 1. More work is needed in future to obtain a better estimate of the entire freshwater supply to Young Sound.

FUTURE CHANGES

The HIRHAM regional model (Christensen and Kuhry, 2000; Christensen et al., 1998; Dethloff et al., 1996) was used to predict changes in wind, temperature, and precipitation minus evaporation (P–E) conditions in East Greenland. The model has a 50-km horizontal resolution and is nested within 2 transient climate-change simulations (Roeckner et al., 1996; Stendel et al., 2000). The ability of the model to simulate realistic present-day arctic conditions has been thoroughly documented (Christensen and Kuhry, 2000; Dethloff et al., 1996). The model predicts small (<5%) changes in the average 30-yr wind conditions in the northeast Greenland region at the end of this century (2071–2100), as compared to present-day (1961–1990) values. In contrast, it predicts a dramatic increase in the average 30-yr atmospheric temperatures of up to 8°C in the region by the end of this century (Fig. 11). Furthermore, the average 30-yr P–E conditions in the region are predicted to increase 20–30% in the same period (Fig. 11). The effect of increased temperatures and P–E can be expected to cause dramatic changes in future sea-ice conditions in Young Sound. Reliable predictions of sea ice changes in Young Sound cannot be made with the HIRHAM model due to insufficient horizontal resolution, but may be made by another approach. Today, sea ice covers the fjord for 9–10 mo of the year and grows to a thickness of ~1.5 m (Fig. 2). Because the water mass underlying the sea ice in

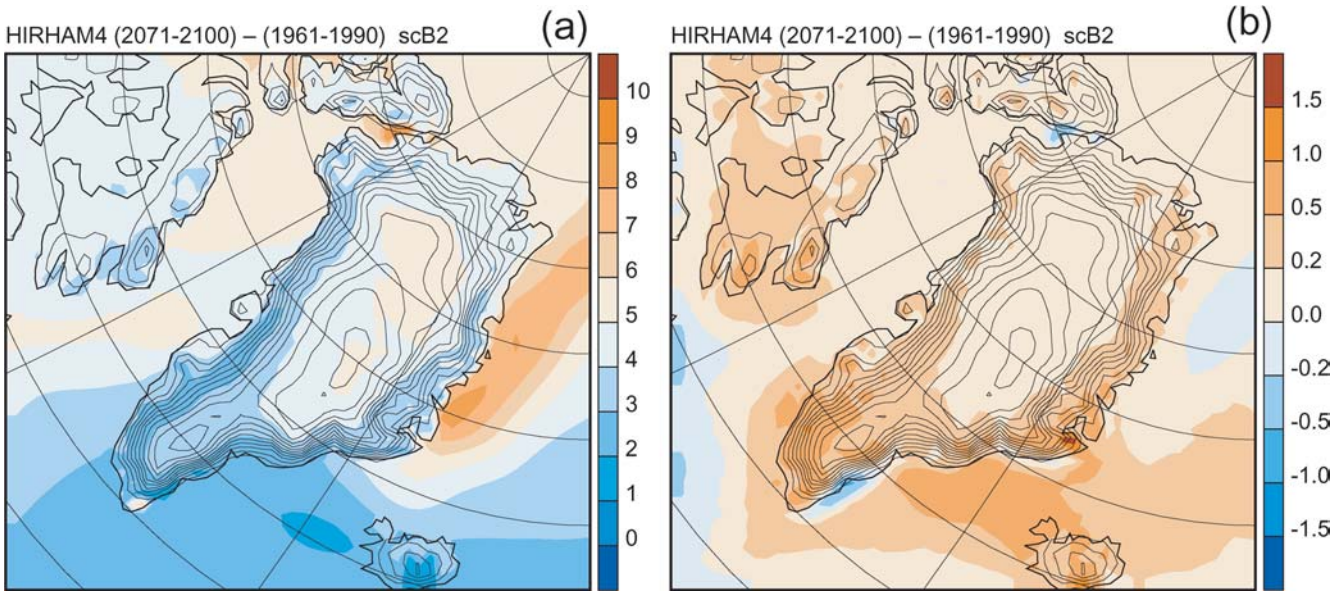

FIGURE 11. (a) Change in 2-m temperatures (°C), and (b) precipitation–evaporation (mm d^{-1}) during 2071–2100 relative to 1961–1990, as estimated by HIRHAM4 scenario B2 simulations. Contour interval shown for every 500 m.

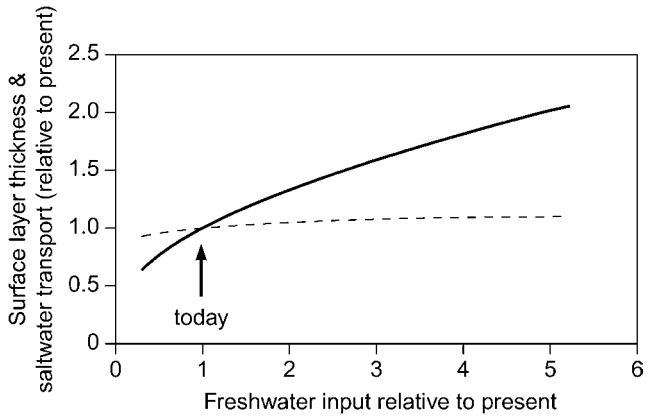

FIGURE 12. Expected changes relative to present conditions in the surface-layer thickness (low-salinity layer in the upper water layers—dotted line) and saltwater transport (Q solid line) in outer Young Sound as a function of freshwater input.

Young Sound consists of polar water, the oceanic heat flux is negligible, and the only factors affecting sea-ice thickness inside the fjord are air temperature and snow cover. Thus, the sea-ice thickness and seasonal length can be estimated from the number of degree-days of freezing since the beginning of winter (Lebedev, 1938; Bilello, 1961), with a further treatment for melt rates in summer (Bilello, 1980). Through this technique and applying the air-temperature rise of 9.3°C ± 1.5 during December–February; 4.7°C ± 1.3 during March–May; 0.4°C ± 0.3 during June–August, and 8.6°C ± 2.1 during September–November predicted by HIRHAM (scenario B2) in 2071–2100, the winter fast-ice thickness in Young Sound can be predicted to decline approximately from 1.4–1.9 (depending on snow thickness) to 0.8–1.3 m, with the expected increase in the ice-free season from 2.5 mo today to 4.7 mo at the end of the century. The scenario A2 data in the estimation further decreases sea-ice thickness and increases the ice-free season to 5.3 mo.

An increased ice-free period will enhance the heat flux from the atmosphere to the surface water and increase the freshwater runoff from land to the fjord. Evaluation of the effect of increased freshwater flux into the fjord according to Officer (1976) reveals that in fjords dominated by entrainment mixing, the surface-layer thickness (e.g., upper low-salinity layer) will change only marginally, whereas the transport of salt water from the Greenland Sea to Young Sound below the halocline will increase significantly due to increased estuarine circulation. (Fig. 12). An increase in the ice-free period will enhance biological productivity in the area due to increased light availability for primary producers (Rysgaard et al., 1999; Kühl et al., 2001; Roberts et al., 2002; Borum et al., 2002; Glud et al., 2002b). Because the surface layer thickness will change only marginally by the end of the century, the phytoplankton bloom will continue to occur in a subsurface layer, but as net transport increases, production will benefit from an increased import of nutrients and organic matter from the Greenland Sea. Improved food availability will stimulate bivalve growth and production in the area (Sejr et al., submitted). Furthermore, an increase in the ice-free season will prolong the period in which birds and marine mammals, e.g., walruses, have access to the food-rich coastal area and thus improve their foraging conditions (Born et al., 2003).

The predicted changes in temperature, ice-free conditions, and precipitation in the area at the end of this century suggest that physical conditions in Young Sound will become more similar to present-day conditions farther south, e.g., at Kap Tobin (Fig. 13). Thus, the area extending from Young Sound and a few hundred km south represents a climate gradient reflecting this century's climate change. We suggest that north-south transects in this region may be highly

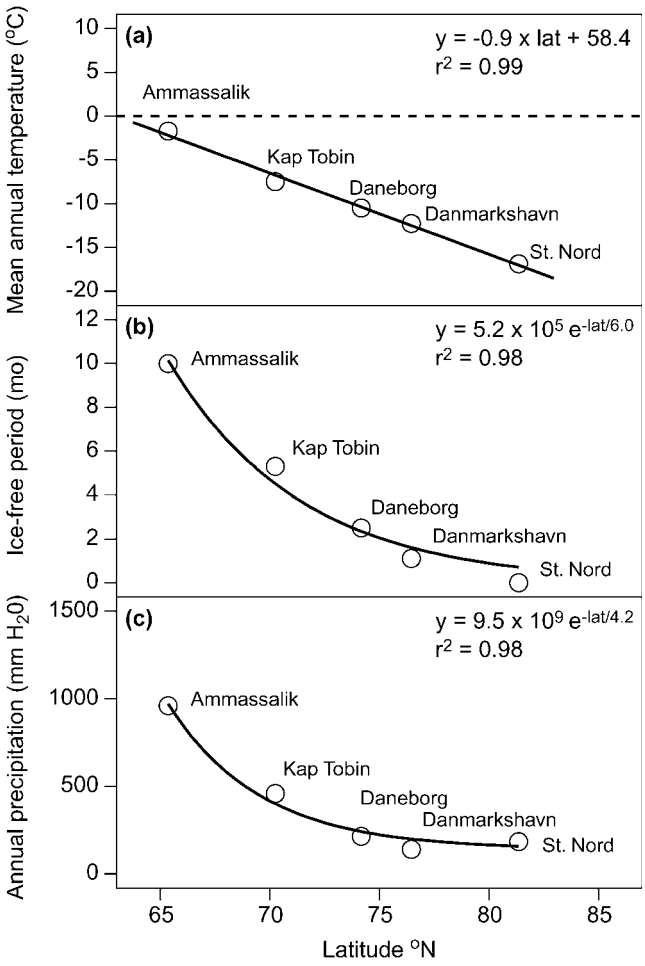

*FIGURE 13. (a) Mean annual temperature in northeast Greenland versus latitude. Data from Capellen et al. (2001). (b) Annual ice-free period versus latitude. Data from the Danish Meterological Institute—*State of the Ice in the Arctic Seas, *annual reports (1950–1964). (c) Mean annual precipitation versus latitude. Data from Ohmura and Reeh (1991). Daneborg is situated in the outer region of Young Sound.*

valuable in evaluating adaptations in biological processes and species to different physical settings in relation to future climate change in the Arctic.

Acknowledgments

The study was supported financially by DANCEA (Danish Cooperation for Environment in the Arctic, Danish Ministry of Environment). We acknowledge the Danish Polar Center for logistical support. The Danish Military Division, Sirius, is thanked for its hospitality. In addition, we wish to thank Egon R Frandsen, Jan Damgaard, Kitte Gerlich, Marlene Skjærbæk, and Tanja Quottrup for technical assistance in the field and laboratory. We thank Ronnie N Glud, Michael Sejr, and Morten Rasch for helpful discussions. Robert Gilbert is thanked for his comments on the manuscript. Finally, we are grateful to Anna Haxen for linguistic corrections.

References Cited

Aure, J., and Stigebrandt, A, 1989: On the influence of topographic factors upon the oxygen consumption rate in sill basin fjords. *Estuarine Coastal Shelf Science,* 28: 59–69.

Bennet, M. R., and Glasser, N. F., 1996: Glacial Geology: Ice Sheets and Landforms. London: John Wiley and Sons Ltd. 364 pp.

Berg, P., Rysgaard S., Funch, P., and Sejr, M. K., 2001: The effects of bioturbation on solutes and solids in marine sediments. *Aquatic Microbial Ecology,* 26: 81–94.

Bilello, M. A., 1961: Formation, growth and decay of sea ice. *Arctic,* 14: 3–24.

Bilello, M. A., 1980: Decay patterns of fast sea ice in Canada and Alaska. *In* Pritchard, R. S. (ed.), *Sea Ice Processes and Model*s ed.:, Seattle: University of Washington Press, 313–326.

Born, E. W., Dietz, R., Heide-Jørgensen, M. P., and Knutsen, L. Ø., 1997: Historical and present status of the Atlantic walrus (*Odobenus rosmarus rosmarus*) in eastern Greenland. *Meddelser Greenland, Bioscience,* 46: 1–73.

Born, E. W., Rysgaard, S., Ehlmé, G., Sejr, M., Acquarone, M., and Levermann, N., 2003: Underwater observations of free-living Atlantic walruses (*Obobenus rosmarus*) with estimates of their food consumption. *Polar Biology.* 26: 348–357.

Borum, J., Pedersen, M. F., Krause-Jensen, D., Christensen, P. B., and Nielsen, K., 2002: Biomass, photosynthesis and growth of *Laminaria saccharina* in a high-arctic fjord, NE Greenland. *Marine Biology,* 141: 11–19.

Braman, R. S., and Hendrix, S. A., 1989: Nanogram nitrite and nitrate determination in environmental and biological meterials by vanadium (III) reduction with chemiluminescence detection. *Analytical Chemistry,* 61: 2715–2718.

Buesseler, K.O., Bauer, J. E., Chen, R. F., Eglinton, T. I., Gustafsson, O., Landing, W., Mopper, K., Moran, S. B., Santschi, P. H., Vernon Clark, R., and Wells, M. L., 1996: An intercomparison of cross-flow filtration techniques used for sampling marine colloids: overview and organic carbon results. *Marine Chemistry,* 55: 1–31.

Cappelen, J., Jørgensen, B. V., Laursen, E. V., Stannius, L. S., and Thomsen, R. S., 2001: *The Observed Climate of Greenland, 1958–99—with Climatological Standard Normals, 1961–90.* Danish Meterological Institute, Copenhagen,. Technical Report 00–18.

Cattle, H., and Crossley, J., 1996: Modelling arctic climate change. *In* Wadhams, P., Dowdeswell, J. A., and Schofield, A. N., (eds.), *The Arctic and Environmental Change.* Cambridge: Gordon and Breach Publishers. 193 pp.

Christensen, J. H., and Kuhry, P., 2000: High resolution regional climate model validation and permafrost simulation for the East-European Russian Arctic. *Journal of Geophysical Research,* 105: 29647–29658.

Christensen, O. B., Christensen, J. H., Machenhauer, B., and Botzet, M., 1998: Very-high-resolution regional climate simulations over Scandinavia: present climate. *Journal of Climate,* 11: 3204–3229.

Cofaigh, C. Ó., Dowdeswell, J. A., and Grobe, H., 2001: Holocene glacimarine sedimentation, inner Scoresby Sund, East Greenland: the influence of fast-flowing ice-sheet outlet glaciers. *Marine Geology,* 175: 103–129.

Dale, J.E., Aitken, A.E., Gilbert, R., and Risk, M.J., 1989: Macrofauna of Canadian arctic fjords. *Marine Geology,* 85: 331–358.

Dethloff, K., Rinke, A., Lehmann, R., Christensen, J. H., Botzet, M., and Machenhauer, B., 1996: Regional climate model of the arctic atmosphere. *Journal of Geophysical Research,* 101: 23401–23422.

Eilertsen, H. C., Falk-Petersen, S., Hopkins, C. C. E., and Tande, K., 1981: Ecological investigations on the plankton community of Balsfjorden, Northern Norway. Program for the project, Study Area, Topography and Physical Environment. *Sarcia,* 66: 25–34.

Escher, A., and Watt, S. (eds.), 1976: *Geology of Greenland.* Copenhagen: Geological Survey of Greenland. 338 pp.

Flato, G. M., and Boer, G. J., 2001: Warming asymmetry in climate change simulations. *Geophysical Research Letters,* 28: 195–198.

Funder, S., 1989: Quaternary geology of the ice-free areas and adjacent shelves of Greenland. *In* Fulton, R. J. (ed.), *Quaternary Geology of Canada and Greenland. Geology of Canada,* no. 1. Ottawa: Geological Survey of Canada, 743–792.

Funder, S., and Hansen, L., 1996: The Greenland ice sheet—a model for its culmination and decay during and after the last glacial maximum. *Bulletin of the Geological Society of Denmark,* 42: 137–152.

Funder, S., Hjort, C., Landvik, J. Y., Nam, S.-I., Reeh, N., and Stein, R., 1998: History of stable ice margin—East Greenland during the middle and upper Pleistocene. *Quaternary Science Reviews,* 17: 77–123.

Gilbert, R., 1983: Sedimentary processes of Canadian arctic fjords. *Sedimentary Geology,* 36: 147–175.

Glud, R. N., Risgaard-Petersen, N., Thamdrup, B., Fossing, H., and Rysgaard, S., 2000: Benthic carbon mineralization in a high arctic sound, (Young Sound, NE Greenland). *Marine Ecology Progress Series,* 206: 59–71.

Glud, R. N., Rysgaard, S., and Kühl, M., 2002a: Oxygen dynamics and photosynthesis in ice algae communities: quantification by microsensors, O_2 exchange rates, ^{14}C-incubations, and PAM-flouremeter. *Aquatic Microbial Ecology,* 27: 301–311.

Glud, R. N., Kühl, M., Wenzhöfer, F., and Rysgaard, S., 2002b: Benthic diatoms of a high arctic fjord (Young Sound NE Greenland): Importance for ecosystem primary production. *Marine Ecology Progress Series,* 238: 15–29.

Grasshoff, K., Erhardt, M., and Kremling, K., 1983: *Methods of Seawater Analysis,* 2nd revised and extended version. Weinheim, Deerfield Beach, Florida, and Basel: Verlage Chemie. 419 pp.

Harrison, W. G., and Cota, G. F., 1991: Primary production in polar waters: relation to nutrient availability. *In* Sakshaug, E., Hopkins, C. C. E., and Øritsland, N. A. (eds.), *Proceedings from the Pro Mare Symposium on Polar Marine Ecology, Tronheim. Polar Research,* 10(1): 87–104.

Johannessen, O. M., Shalina, E. V., and Miles, M. W., 1999: Satellite evidence for an arctic sea ice cover in transformation. *Science,* 286: 1937–1939.

Knudsen, M., 1900: Ein hydrographischer Lehrsatz. *Annalen der Hydrographie und Maritimen Meteorologie,* 28: 316–320. (In German.)

Kühl, M., Glud, R. N., Borum, J., Roberts, R., and Rysgaard, S., 2001: Photosynthetic performance of surface associated algae below sea ice as measured with a pulse amplitude modulated (PAM) fluorometer and O_2 microsensors. *Marine Ecology Progress Series,* 223: 1–14.

Lebedev, V. V., 1938: Rost l'do v arkticheskikh rekakh i moriakh v zavisimosti ot otritsatel'nykh tempertur vozdukha. *Problemy Arktiki,* 5: 9–25.

Levinsen, H., Turner, J. T., Nielsen, T. G., and Hansen, B. W., 2000: On the trophic coupling between protists and copepods in arctic marine ecosystems. *Marine Ecology Progress Series,* 204: 65–77.

Levitus, S., Antonov, J. I., Boyer, T. P., and Stephens, C., 2000: Warming of the world ocean. *Science,* 287: 2225–2229.

Manabe, S., and Stouffer, R. J., 1993: Century-scale effects of increased atmospheric CO_2 in the ocean-atmosphere system. *Nature,* 364: 215–218.

Meltofte, H., and Rasch, M. (eds.), 1998: *ZERO—Zackenberg Ecological Research Operations. 3rd Annual Report 1997.* Copenhagen: Danish Polar Center. Ministry of Research and Information Technology. 68 pp.

Meltofte, H., and Thing, H. (eds.), 1996: *ZERO—Zackenberg Ecological Research Operations. 1st Annual Report 1995.* Copenhagen: Danish Polar Center. Ministry of Research and Information Technology. 64 pp.

Meltofte, H., and Thing, H. (eds.), 1997: *ZERO—Zackenberg Ecological Research Operations. 2nd Annual Report 1996.* Copenhagen: Danish Polar Center. Ministry of Research and Information Technology. 80 pp.

Nielsen, N., and Rasch, M., 1997: Coastal geomorphology and fjord sedimentology. *In* Meltofte, N., and Thing, H. (eds.), *ZERO—Zackenberg Ecological Research Operations, 2nd Annual Report, 1996.* Copenhagen: Danish Polar Center, Ministry of Research and Information Technology. 80 pp.

Officer, C. B., 1976: *Physical Oceanography of Estuaries (and Associated Coastal Waters).* New York: John Wiley and Sons. 465 pp.

Officer, C. B., 1980: Box models revisited. *In* Hamilton, P., and Macdonald, K. B. (eds.), *Estuarine and Wetland Processes*. London: Plenum Press, 65–114.

Ohmura, A., and Reeh, N., 1991: New precipitation and accumulation maps for Greenland. *Journal of Glaciology,* 37: 140–148.

Parkinson, C. L., 1992: Spatial patterns of increases and decreases in the length of the sea ice season in the North Pole Region, 1979–1986. *Journal of Geophysical Research,* 97: 14377–14388.

Rasch, M. (ed.), 1999: *ZERO—Zackenberg Ecological Research Operations. 4th Annual Report 1998*. Copenhagen: Danish Polar Center. Ministry of Research and Information Technology. 62 pp.

Rasch, M., Elberling, B., Jakobsen, B. H., and Hasholt, B., 2000: High-resolution measurements of water discharge, sediment, and solute transport in the River Zackenbergelven, northeast Greenland. *Arctic, Antarctic, and Alpine Research,* 32: 336–345.

Rasmussen, B., 1997: The near-surface horizontal buoyancy flux in a highly stratified region, Kattegat. *Estuarine, Coastal and Shelf Science,* 45: 405–414.

Rasmussen, B., and Josefson, A. B., 2002: Consistent estimates for the residence time of micro-tidal estuaries. *Estuarine, Coastal and Shelf Science,* 54: 65–73.

Roberts, R., Glud, R. N., Kühl, M., and Rysgaard, S., 2002: Primary production of crustose coralline red algae in a high arctic fjord. *Journal of Phycology,* 38: 1–11.

Roeckner, E., Arpe, K., Bengtsson, L., Christoph, M., Claussen, M., Dümenil, L., Esch, M., Giorgetta, M., Schlese, U., and Schulzweida, U., 1996: *The Atmospheric General Circulation Model ECHAM-4: Model Description and Simulation of Present-Day Climate*. Hamburg: Max Planck Institute für Meteorologie Report 218. 90 pp.

Rysgaard, S., Dahlgaard, H., and Finster, K., 1996: Primary production, nutrient dynamics and mineralization in a northeastern Greenland fjord during the summer thaw. *Polar Biology,* 16: 497–506.

Rysgaard, S., Thamdrup, B., Risgaard-Petersen, N., Fossing, H., Berg, P., Christensen, P. B., and Dalsgaard, T., 1998: Seasonal carbon and nitrogen mineralization in a high-arctic coastal marine sediment, Young Sound, northeast Greenland. *Marine Ecology Progress Series,* 175: 261–276.

Rysgaard, S., Nielsen, T.G., and Hansen, B., 1999: Seasonal variation in nutrients, pelagic primary production and grazing in a high-arctic coastal marine ecosystem, Young Sound, northeast Greenland. *Marine Ecology Progress Series,* 179: 13–25.

Rysgaard, S., Kühl, M., Glud, R. N., and Hansen, J. W., 2001: Biomass, production, and horizontal patchiness of sea ice algae in a high-arctic fjord (Young Sound, NE-Greenland). *Marine Ecology Progress Series,* 223: 15–26.

Sejr, M. K., Jensen, K. T., and Rysgaard, S., 2000: Macrozoobenthos in a northeast Greenland fjord: structure and diversity. *Polar Biology,* 23: 792–801.

Sejr, M. S., Petersen, J.K., Jensen, K. T., and Rysgaard, S., submitted: Effects of food concentration on clearance rate and energy budget of the arctic bivalve *Hiatella arctica* (L) at sub-zero temperature. *Marine Ecology Progress Series*

Sejr, M. K., Sand, M. K., Jensen, K. T., Petersen, J. K., Christensen, P. B., and Rysgaard, S., 2002: Growth and production of *Hiatella arctica* (Bivalvia) in high arctic Young Sound, northeast Greenland. *Marine Ecology Progress Series,* 244: 163–169.

Serreze, M. C., Walsh, J. E., Chapin, F. S., III, Osterkamp, T., Dyurgerov, M., Romanovsky, V., Oechiel, W. C., Morison, J., Xhang, T., and Barry, R. G., 2000: Observational evidence of recent changes in the northern high-latitude environment. *Climatic Change,* 46: 159–207.

Shindell, D. T., Miller, R. L., Schmidt, G. A., and Pandolfo, L., 1999: Simulation of recent northern winter climate trends by greenhouse-gas forcing. *Nature,* 399: 452–455.

Soegaard, H., Hasholt, B., Friborg, T., and Nordstroem, C., 2001: Surface energy and water balance in a high-arctic environment in NE Greenland. *Theoretical and Applied Climatology,* 70: 35–51.

Stendel, M., Schmith, T., Roeckner, E., and Cubasch, U., 2000: *The Climate of the 21st Century: Transient Simulations with a Coupled-Atmosphere-Ocean General Circulation Model*. Copenhagen: Danish Climate Centre Report 00–6. 51 pp.

Sugden, D. E., 1974: Landscapes of glacial erosion in Greenland and their relationship to ice, topographic and bedrock conditions. *Institute of British Geographers, Special Publications* 7: 177–195.

Ms submitted July 2002